
Quantitative Comparison and Analysis of Species-Specific Wound Biofilm Virulence Using an In Vivo, Rabbit-Ear Model

Akhil K Seth, MD, Matthew R Geringer, BS, Robert D Galiano, MD, Kai P Leung, PhD, Thomas A Mustoe, MD, FACS, Seok J Hong, PhD

- BACKGROUND:** Although bacterial biofilm is recognized as an important contributor to chronic wound pathogenesis, differences in biofilm virulence between species have never been studied in vivo.
- STUDY DESIGN:** Dermal punch wounds in New Zealand white rabbit ears were inoculated with *Klebsiella pneumoniae*, *Staphylococcus aureus*, or *Pseudomonas aeruginosa*, or left uninfected as controls. In vivo biofilm was established and maintained using procedures from our previously published wound biofilm model. Virulence was assessed by measurement of histologic wound healing and host inflammatory mediators. Scanning electron microscopy (SEM) and bacterial counts verified biofilm viability. Extracellular polymeric substance (EPS)-deficient *P aeruginosa* was used for comparison.
- RESULTS:** SEM confirmed the presence of wound biofilm for each species. *P aeruginosa* biofilm-infected wounds showed significantly more healing impairment than uninfected, *K pneumoniae*, and *S aureus* ($p < 0.05$), while also triggering the largest host inflammatory response ($p < 0.05$). Extracellular polymeric substance-deficient *P aeruginosa* demonstrated a reduced impact on the same quantitative endpoints relative to its wild-type strain ($p < 0.05$).
- CONCLUSIONS:** Our novel analysis demonstrates that individual bacterial species possess distinct levels of biofilm virulence. Biofilm EPS may represent an integral part of their distinct pathogenicity. Rigorous examination of species-dependent differences in biofilm virulence is critical to developing specific therapeutics, while lending insight to the interactions within clinically relevant, polybacterial biofilms. (J Am Coll Surg 2012;215:388–399. © 2012 by the American College of Surgeons)
-

Bacterial biofilms, defined as a surface-adhered, complex community of aggregated bacteria within a matrix of extracellular polymeric substance (EPS), are increasingly being recognized as an integral component of chronic wound

pathogenesis.¹⁻⁷ Given the enormous burden that these wounds place on patients and the health care system,⁸⁻¹⁴ continued research aimed at delineating the mechanisms associated with wound biofilm development and maintenance remains critical. In particular, recent clinical studies have suggested that the predominant bacteria within a chronic wound can be one of several different species, and can often be present as polybacterial biofilm infections.^{2,4,7,15} These findings are supplemented by studies that have demonstrated the formation of biofilm by different bacterial species, including *Staphylococcus aureus*,¹⁶⁻¹⁸ *Pseudomonas aeruginosa*,¹⁹⁻²¹ and *Staphylococcus epidermidis*,²²⁻²⁴ in a variety of in vivo model systems. The potential for wound biofilms to originate from different, or multiple, bacterial species further complicates our limited understanding, indicating a need to examine biofilm pathophysiology at a species-specific level.

Biofilm-phase bacteria can be distinguished from their free-floating, “planktonic” counterparts by their inherent defense and survival mechanisms. The biofilm EPS provides a physical barrier against inflammatory cell phagocytosis, while also po-

Disclosure Information: Nothing to disclose.

This work was supported by the US Army Medical Research and Materiel Command.

Disclaimer: The opinions or assertions contained herein are the private views of the author and are not to be construed as official or as reflecting the views of the Department of the Army or the Department of Defense.

Presented at the Wound Healing Society Annual Meeting, Dallas, TX, April 2011.

Drs Seth and Geringer contributed equally to this work.

Received January 25, 2012; Revised May 21, 2012; Accepted May 21, 2012. From the Division of Plastic Surgery, Feinberg School of Medicine, Northwestern University, Chicago, IL (Seth, Geringer, Galiano, Mustoe, Hong) and the Microbiology Branch, US Army Dental and Trauma Research Detachment, Institute of Surgical Research, Fort Sam Houston, TX (Leung).

Correspondence address: Seok J Hong, PhD, Feinberg School of Medicine, Northwestern University, 300 East Superior St, Tarry 4-723, Chicago, IL 60611. email: seok-hong@northwestern.edu

Report Documentation Page

Form Approved
OMB No. 0704-0188

Public reporting burden for the collection of information is estimated to average 1 hour per response, including the time for reviewing instructions, searching existing data sources, gathering and maintaining the data needed, and completing and reviewing the collection of information. Send comments regarding this burden estimate or any other aspect of this collection of information, including suggestions for reducing this burden, to Washington Headquarters Services, Directorate for Information Operations and Reports, 1215 Jefferson Davis Highway, Suite 1204, Arlington VA 22202-4302. Respondents should be aware that notwithstanding any other provision of law, no person shall be subject to a penalty for failing to comply with a collection of information if it does not display a currently valid OMB control number.

1. REPORT DATE 01 SEP 2012		2. REPORT TYPE N/A		3. DATES COVERED -	
4. TITLE AND SUBTITLE Quantitative Comparison and Analysis of Species-Specific Wound Biofilm Virulence Using an In Vivo, Rabbit-Ear Model				5a. CONTRACT NUMBER	
				5b. GRANT NUMBER	
				5c. PROGRAM ELEMENT NUMBER	
6. AUTHOR(S) Seth A. K., Geringer M. R., Galiano R. D., Leung K. P., Mustoe T. A., Hong S. J.,				5d. PROJECT NUMBER	
				5e. TASK NUMBER	
				5f. WORK UNIT NUMBER	
7. PERFORMING ORGANIZATION NAME(S) AND ADDRESS(ES) United States Army Institute of Surgical Research, JBSA Fort Sam Houston, TX				8. PERFORMING ORGANIZATION REPORT NUMBER	
9. SPONSORING/MONITORING AGENCY NAME(S) AND ADDRESS(ES)				10. SPONSOR/MONITOR'S ACRONYM(S)	
				11. SPONSOR/MONITOR'S REPORT NUMBER(S)	
12. DISTRIBUTION/AVAILABILITY STATEMENT Approved for public release, distribution unlimited					
13. SUPPLEMENTARY NOTES					
14. ABSTRACT					
15. SUBJECT TERMS					
16. SECURITY CLASSIFICATION OF:			17. LIMITATION OF ABSTRACT UU	18. NUMBER OF PAGES 12	19a. NAME OF RESPONSIBLE PERSON
a. REPORT unclassified	b. ABSTRACT unclassified	c. THIS PAGE unclassified			

Abbreviations and Acronyms

CFU	= colony-forming unit
EPS	= extracellular polymeric substance
POD	= postoperative day
qRT-PCR	= quantitative reverse transcription-polymerase chain reaction
SEM	= scanning electron microscopy

tentially inhibiting the complement cascade and the activation and penetration of antibiotics.^{22,25-28} Others have suggested that the shedding of planktonic bacteria and the maintenance of phenotypically distinct “persister” cells contribute to its sustainability and durability within the hostile environment of its host surface.^{2,3} However, some protective mechanisms have been frequently linked to certain bacterial species more than others. Cell-to-cell signaling, termed *quorum-sensing*, has been implicated as a major component of *P aeruginosa* biofilm pathogenicity both in vitro and in vivo,^{2,21,29,30} while it remains controversial in *S aureus*.³¹ Meanwhile, several different regulatory molecules have been identified as important to the biofilm-forming ability of *S aureus*, including *sarA*,^{32,33} *agr*,³⁴ and *cidA*.³⁵ As part of mediating resistance to neutrophils, *S epidermidis* biofilms use an intracellular adhesin to prevent phagocytosis, while *P aeruginosa* biofilms may diminish the neutrophils’ oxidative potential^{36,37} or lead to their rapid necrosis through rhamnolipid production.³⁸ Therefore, although the biofilm phenotype is common to most bacteria, individual bacterial species may use different mechanisms to achieve and maintain their presence within a wound.

Although the aforementioned differences in species-specific biofilms have been established, the end effects of each species’ biofilm on wounds and their host, ie, virulence, are unclear. Clinical observation suggests that differences in biofilm virulence exist, as the appearance and severity of wounds can often be linked to one bacterial species over another based on experience. Unfortunately, these conclusions rely on anecdotal evidence rather than rigorous scientific experimentation. There remains no study in the literature, to date, that has evaluated and compared the species-specific virulence of different bacterial wound biofilms. Understanding species-dependent differences in biofilm pathogenicity may contribute to the development of specific, targeted biofilm therapeutics, while also lending insight to the interactions that occur within a polybacterial setting.

The goal of this study was to use our established, rabbit ear, wound biofilm model¹⁶ to investigate whether there are differences in biofilm virulence across multiple bacterial species. Through comparison of the common wound pathogens *K pneumoniae*, *S aureus*, and *P aeruginosa*, we

have discovered and attributed a distinct level of virulence to each species. In line with clinical observation, we demonstrated that *P aeruginosa* biofilm has the most significant effect on wound healing and the host inflammatory response. We investigated the mechanism of this pathogenicity using a mutant *P aeruginosa* strain. In doing so, we implicated the EPS as a critical contributor to *Pseudomonas* virulence, which has not been previously reported. With these results, we also validate the sensitivity of our in vivo system, establishing the model as a valuable and informative tool for translational biofilm research.

METHODS**Animals**

Under an approved protocol by the Animal Care and Use Committee at Northwestern University, adult New Zealand white rabbits (3 to 6 months old, approximately 3 to 4 kg) were acclimated to standard housing and fed ad libitum. All animals were housed in individual cages under constant temperature and humidity with a 12-hour light-dark cycle. A total of 26 rabbits were used to complete this study.

Bacterial species

Three separate bacterial species were used including individual strains of *K pneumoniae* (BAMC 07-18), *S aureus* (UAMS-1), and *P aeruginosa* (PAO1 and mutant strain *pelApslBCD*). The *K pneumoniae* strain BAMC 07-18 (kindly provided by LTC Clinton Murray of Brooke Army Medical Center, Fort Sam Houston, TX) was originally isolated from the wounds of an injured soldier that had returned from Iraq during the war. PAO1 was obtained from the laboratory of Dr Barbara H Iglewski (University of Rochester Medical Center). *P aeruginosa* mutant *pelApslBCD* was kindly provided by Dr Tim Tolker-Nielsen of the University of Copenhagen. The *pelApslBCD* mutant is a previously characterized double mutant of the *pel* and *psl* loci mutants, each of which causes deficiencies in the biosynthesis of polysaccharides that are part of *P aeruginosa* EPS.

To prepare bacterial culture each species was grown on specific agar plates (Hardy Diagnostics; BAMC 07-18 on blood agar, UAMS-1 on *S aureus* isolation agar, PAO1 and *pelApslBCD* on *P aeruginosa* isolation agar) overnight at 37°C. Each species was then subcultured at 37°C into 10 mL of tryptic soy broth (TSB; BAMC 07-18 and UAMS-1) or Luria broth (LB; *P aeruginosa* strains) and grown at 37°C until log-phase was achieved. Bacteria were harvested and washed in phosphate-buffered saline (PBS) once by centrifugation at 5,000 rpm for 5 minutes at 20°C. The resultant pellet was resuspended in PBS and an optical density at the 600-nm wavelength (OD₆₀₀) was measured. For each species, an OD₆₀₀ equivalent to 10⁶ colony-forming units (CFU)/μL was determined pre-empirically.

Table 1. Study Design and Wound Distribution per Study Group

Analysis endpoint	5 rabbits (n = 60 wounds)			
	Rabbits: 1, 2 (POD 6) (n = 24 wounds)		Rabbits: 3, 4, 5 (POD 12) (n = 36 wounds)	
	Left ears (n = 12)	Right ears (n = 12)	Left ears (n = 18)	Right ears (n = 18)
qRT-PCR	6	6		
Bacterial counts	6	6		
SEM			6	6
Histology			12	12

Data presented as number of wounds (1 rabbit had 12 wounds, 6 wounds/ear). Study groups: control, *K pneumoniae*, *S aureus*, *P aeruginosa*, *pelApslBCD*. POD, postoperative day; qRT-PCR, quantitative reverse transcription-polymerase chain reaction; SEM, scanning electron microscopy.

Wound protocol and infection model

Rabbits were anesthetized with intramuscular injection of a ketamine (22.5 mg/kg) and xylazine (3.5 mg/kg) mixture before surgery. Ears were shaved, sterilized with 70% ethanol, and injected intradermally with 1% lidocaine/1:100,000 epinephrine at the planned wound sites. Six, 6-mm diameter, full-thickness dermal wounds were created on the ventral side of each ear, totaling 12 wounds per rabbit, down to perichondrium and dressed with Tegaderm (3M Health Care), a semioclusive transparent film. Individual wounds were either left sterile as uninfected controls or inoculated with 10^6 CFU of an individual test bacteria strain on postoperative day (POD) 3. Each rabbit was designated as a control or was infected with only bacterial species, with no cross-contamination of bacteria within or between ears. For each study group, 60 wounds (5 rabbits) were used for data analysis, totaling 300 wounds (25 rabbits; Table 1). Because we had no previous experience using the *P aeruginosa* mutant strain *pelApslBCD*, an additional animal was inoculated with *pelApslBCD* to ensure feasibility and animal safety, but was not included in any analyses.

Bacteria were allowed to proliferate under the Tegaderm dressing. Topical Mupirocin (2%; Teva Pharmaceuticals) or Ciloxan (Ciprofloxacin 0.3%, Alcon) antibiotic ointment was applied on postoperative day (POD) 4 to *S aureus* and *K pneumoniae* or *P aeruginosa* infected wounds, respectively, to eliminate free-floating, planktonic-phase bacteria, leaving a predominately biofilm-phase phenotype. To prevent seroma formation and regrowth of planktonic bacteria, therefore maintaining a biofilm-dominant infection, an antimicrobial, absorbent dressing containing polyhexamethylene biguanide (Telfa AMD, Tyco Healthcare Group) was applied to biofilm wounds on PODs 5 and 6, and then every other day until harvest. An overlying Tegaderm dressing was maintained throughout the protocol, and all dressings were checked daily.

Harvesting of wounds

After euthanizing animals by intracardiac euthasol injection, wounds were harvested for various analyses at different time points. Wounds for histologic analysis using hematoxylin and eosin (H&E) staining, and scanning electron microscopy (SEM) to visualize biofilm morphology, were harvested at POD 12. For quantitative reverse transcription-polymerase chain reaction (qRT-PCR) analysis to measure inflammatory cytokine mRNA levels, and viable bacterial counts, wounds were harvested on POD 6. For each analysis endpoint, wounds were taken from both ears from multiple animals (eg, qRT-PCR: 3 wounds from the left ear and 3 wounds from the right ear from rabbits 1 and 2; Table 1) to account for any potential inherent variability between rabbits. All wounds were excised using a 10-mm (histology, SEM, viable bacterial counts) or 7-mm (qRT-PCR) biopsy punch (Acuderm Inc). Wounds were omitted from the final results if difficulties were encountered during tissue handling or processing that prevented appropriate or consistent analysis.

Histologic analysis

Wounds excised for histologic analysis were bisected at their largest diameter for hematoxylin and eosin staining. Tissues were fixed in formalin, embedded in paraffin, and cut into 4- μ m sections. Paraffin was removed with a xylene wash, followed by a standard hematoxylin and eosin staining protocol to prepare samples for analysis under a light microscope. Slides were examined for quantification of epithelial and granulation gaps, and total granulation area, using a digital analysis system (NIS-Elements Basic Research, Nikon Instech Co), as previously described.³⁹ In brief, epithelial and granulation gaps were measured as the distance between the distal leading edges of any newly formed epithelial and granulation tissue, respectively. New granulation tissue area was defined as the sum of the granulation tissue in-growth areas on either side of the wound, inside of the 6-mm wound border. The wound border was determined histologically by the "nick" in the cartilage on either side of the wound bed and/or visual differences in the

tissue between existing dermis and newly formed granulation tissue. Two blinded, independent observers evaluated all histologic sections. The results of both examiners were averaged. Slides were omitted if results differed more than 30% among examiners.

Scanning electron microscopy

To determine biofilm structure, wound samples were fixed in 2.5% glutaraldehyde in 0.1 M (pH 7.2), washed 3 times in PBS, and dehydrated through an ethanol series and hexamethyldisilazane. Samples were mounted by double-sided tape to specimen stubs, followed by gold-platinum (50:50) ion coating (108 Auto Sputter Coater, TedPella, Inc). Wounds for SEM had their dorsal sides removed before preparation to allow for better mounting for visualization. Samples were visualized using a Carl Zeiss EVO-40 scanning electron microscope operated at the scanning voltage of 10 kV. Sterile control wounds were used as a baseline for visual comparison against infected wounds.

Total mRNA extraction and quantitative reverse-transcription polymerase chain reaction

The dermal layer on the dorsal side of the ear was removed for wounds harvested for mRNA extraction and subsequent cDNA conversion as part of qRT-PCR. Wounds were excised using a 7-mm punch, with an original 6-mm wound bed, leaving a 0.5-mm diameter rim of normal skin around the wound bed. Based on previous work with this model,¹⁶ harvest for mRNA extraction was done on POD 6. At this time, a steady-state of biofilm-phase bacteria is thought to be present after topical antibiotic and Telfa dressing placement, triggering the largest inflammatory response. Wounds were immediately snap-frozen in liquid nitrogen after excision. Before mRNA extraction, wound samples were homogenized using a Mini-bead beater-8 (Biospec Products Inc) with zirconia beads (2.0 mm diameter, Biospec Products Inc) in the presence of Trizol Reagent (Sigma-Aldrich). Total RNA was isolated according to the manufacturer's protocol. Contaminating genomic DNA during RNA preparation was removed using the Turbo DNA-free kit (Ambion). Five- μ g of total RNA was used to prepare cDNA using superscript II (Invitrogen) with 100 ng of random primers (Invitrogen).

For quantitative analysis of the level of mRNAs, qPCR analyses using SYBR green 1 were performed using an ABI prism 7000 sequence detection system (Applied Biosystems). Polymerase chain reaction primers were designed using the Primer 3 program (<http://frodo.wi.mit.edu/>). Expression of each gene was normalized to the level of glyceraldehyde 3-phosphate dehydrogenase (Gapdh), the house keeping gene, to get Δ Ct. The $2^{-\Delta\Delta C_t}$ method was used to

calculate mRNA levels of interleukin (IL)-1 β and tumor necrosis factor (TNF)- α within the wounds of interest. Expression of genes was detected by PCR with the following oligonucleotides: IL-1 β (forward: 5'-CCACAGTGGCAATGAAAATG-3' and reverse: 5'-AGAAAGTTCTCAGGCCGTCA-3', accession number D21835), TNF- α (forward: 5'-CCAGATGGTCACCCTCAGAT-3' and reverse: 5'-TGT-TCTGAGAGGCGTGATTG-3', accession number M12845), Gapdh (forward: 5'-AGGTCATCCACGACCACTTC-3' and reverse: 5'-GTGAGTTTCCCGTTCAGCTC-3', accession number NM_001082253). Values were then further normalized by expressing the mRNA level as a fold-difference over the level seen in nonwounded skin. Nonwounded skin was obtained from ears of control animals designated for qRT-PCR.

Viable bacterial counts

The dorsal side of wounds used for bacterial counts were removed to eliminate the inclusion of bacteria outside of the infected wound surface. These wounds were harvested on POD 6 to correlate the qRT-PCR results with the extent of bacterial burden seen in each wound. To recover bacteria, infected wound samples were placed in tubes prefilled with homogenizer beads (Roche). One mL of PBS was added and the tube was homogenized for 90 seconds at 5,000 rpm in a MagnaLYSER homogenizer (Roche) and then sonicated (Microson Ultrasonic Cell Disrupter, Heat Systems-Ultrasonics, Inc) for 2 minutes at 6 to 8 watts to disrupt biofilms and release any bacteria present within the structures. For each bacterial species, the resulting solutions were serially diluted and plated on the appropriate agar plates, as used during bacterial culturing. Plates were incubated overnight at 37°C. Colony forming units were determined by standard colony counting method. Control wounds designated for "bacterial counts" were plated to ensure baseline sterility of wounds relative to those inoculated with a specific bacteria.

Statistical analysis

Data are presented in graphic form as mean \pm standard errors when applicable. Statistical analyses were performed using the Student's *t*-test (2-tailed, unpaired) when comparing 2 study groups, and 1-way analysis of variance (ANOVA) when comparing the means of multiple groups. The level of significance was set at $p < 0.05$.

RESULTS

To validate the presence of biofilm-phase bacteria within our wounds, SEM imaging was performed for each bacterial species (Fig. 1). In each case, wounds revealed the presence of the inoculated bacteria throughout the wound bed.

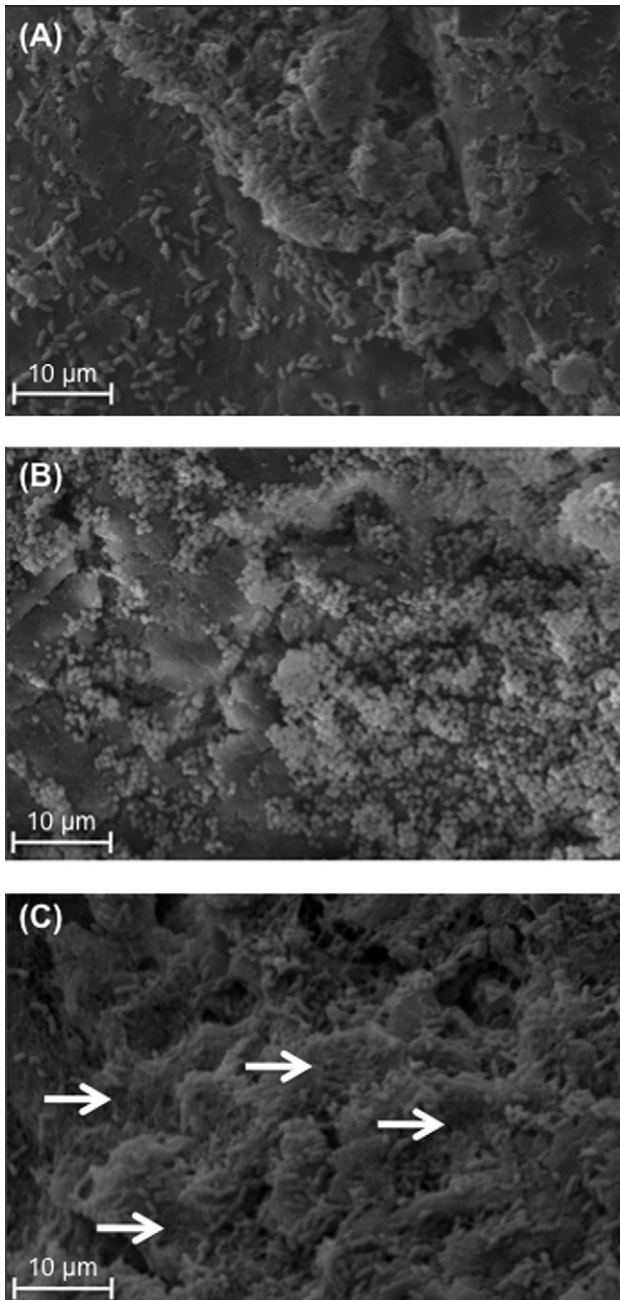


Figure 1. Scanning electron microscopy images of wound biofilms from each bacterial species studied. (A) *K pneumoniae* and (B) *S aureus* wounds revealed clustering of rod- and cocci-shaped bacterial cells, respectively, on the wound surface with minimal amounts of extracellular polymeric substance (EPS) matrix components between cells. (C) *P aeruginosa* wounds demonstrated smaller numbers of cells with large amounts of lattice-like EPS matrix (arrows) interspersed between bacteria.

K pneumoniae wounds demonstrated characteristic rod-shaped bacteria with some cells in clusters, typical of biofilm morphology (Fig. 1A). Similar patterns were verified with the cocci-shaped *S aureus* (Fig. 1B) and rod-shaped *P aeruginosa* (Fig. 1C) wounds. However, *P aeruginosa* wounds tended to possess a higher density of EPS material as compared with *K pneumoniae* and *S aureus*. This EPS appeared organized into a well-defined matrix and interspersed within clusters of *P aeruginosa* cells.

Having verified the consistency of our in vivo model to form biofilm across multiple bacterial species, an analysis of each species' effects on wound healing was performed. Gross appearance of biofilm-infected wounds revealed distinct differences in wound healing at POD 12 (Figs. 2A to 2C). In particular, *P aeruginosa* wounds demonstrated an overall greater impairment in healing as compared with both *S aureus* and *K pneumoniae*. Notable differences also existed between *S aureus* and *K pneumoniae*, with *K pneumoniae* consistently having the largest amount of healing. This hierarchy of wound healing inhibition between species was further supported by histologic analysis (Figs. 2D to 2F). *K pneumoniae* wounds appeared to have the largest amount of epithelial and granulation tissue among the 3 species (Fig. 2D); *P aeruginosa* imparted the greatest inhibitory effect over the same time period (Fig. 2F). Quantification of these histologic parameters revealed statistically significant differences between *P aeruginosa* biofilm-infected wounds and uninfected, *K pneumoniae*, and *S aureus* wounds in both wound epithelialization and granulation ($p < 0.05$; Fig. 3). Furthermore, the incremental progression in virulence was maintained when averaged across multiple wounds ($n = 16$ to 20 wounds/species), progressing from *K pneumoniae* to *S aureus* to *P aeruginosa*.

Individual bacteria species' virulence was further assessed through measurement of the extent of host inflammatory response to each species. The mRNA levels of inflammatory cytokines IL-1 β and TNF- α were measured through qRT-PCR for each species, followed by normalization to the level seen in nonwounded skin (Figs. 4A, 4B). For both cytokines, *P aeruginosa* demonstrated significantly higher levels of mRNA as compared with the other 2 species ($p < 0.05$), indicating a relatively heightened inflammatory response to the presence of *P aeruginosa* biofilm within wounds. Viable bacterial counts were then performed at the same time point to ensure that differences in the host response were not related to measurable differences in bacterial burden (Fig. 4C). There were no differences in viable bacteria levels between *K pneumoniae* and *S aureus*. However, *P aeruginosa* wounds had significantly lower viable bacteria counts ($p < 0.01$) across all wounds ($n = 8$ to 10 wounds/species) than *K pneumoniae* or

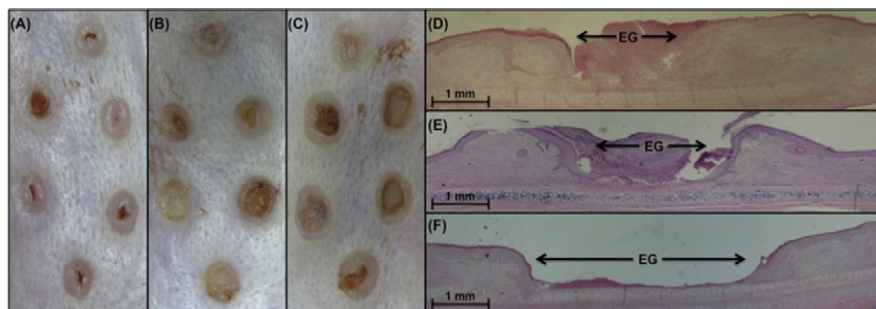


Figure 2. Gross appearance and histologic sections of biofilm-infected wounds at the time of harvest from each bacterial species studied. In general, at postoperative day (POD) 12, (A) *K pneumoniae* wounds demonstrated the largest amount of gross wound healing. In comparison, (B) *S aureus* and (C) *P aeruginosa* wounds appeared to have larger gaps in epithelialization and less wound bed granulation. Correlating with their gross appearance, histologic sections stained with hematoxylin and eosin at POD 12 show that (D) *K pneumoniae* had the greatest amount of new epithelial and granulation tissue in-growth. (E) *S aureus* appeared to have a larger epithelial gap in comparison to *K pneumoniae*. However, (F) *P aeruginosa* showed the largest amount of wound healing impairment among the 3 bacterial species studied. (Magnification $\times 20$) EG, epithelial gap.

S aureus, despite triggering the largest inflammatory response among all 3 species.

The impressive virulence of *P aeruginosa*, relative to *K pneumoniae* and *S aureus*, prompted further investigation into the potential mechanism(s) contributing to these differences. Given the density of EPS in *P aeruginosa* wounds relative to the other 2 species studied, further experiments were performed using the *P aeruginosa* EPS-deficient mutant *pelAps/BCD* to investigate EPS' potential role in *P aeruginosa* virulence. Scanning electron microscopy of wounds infected with the *pelAps/BCD* mutant bacteria verified the expression of an EPS-deficient phenotype, with a distinct lack of polymeric substance components between bacterial cells as compared with the PAO1 wild-type strain (Fig. 5). However, despite the deficiency in EPS, *pelAps/BCD* mutants did demonstrate some bacterial clustering, as would be expected by biofilm-phase bacteria (Figs. 5C, 5D).

Differences in virulence between wild-type PAO1 and the EPS-deficient mutant *pelAps/BCD* were assessed using the endpoints previously described for comparing *K pneumoniae* and *S aureus* with *P aeruginosa*. The gross appearance of *pelAps/BCD*-infected wounds revealed improved healing relative to PAO1-infected wounds (Figs. 6A, 6B). This result was also seen on histologic comparison, with visual (Figs. 6C, 6D) and quantitative (Fig. 7) differences in the extent of wound healing inhibition between the wild-type and mutant strains of *P aeruginosa*. Measurement of inflammatory cytokine mRNA levels corroborated these differences in virulence, with a significantly lower host response to the presence of the *pelAps/BCD* mutant in the wound ($p < 0.05$; Figs. 8A, 8B). The number of viable bacteria in *pelAps/BCD*-infected wounds was equivalent to that of

PAO1 wounds (Fig. 8C), indicating that the differences in inflammatory cytokine expression were inherent to the bacterial strains themselves.

DISCUSSION

Understanding bacterial biofilm pathogenicity remains essential to developing effective treatment strategies for chronic wounds. With several resistance mechanisms and its dynamic response to environmental cues such as in wounds, the ability of biofilm to originate from one of several different bacterial species only increases its complexity. Although many principles of biofilm dynamics are conserved across bacterial species, potential differences in biofilm virulence between species have not been studied. Using an established, in vivo wound biofilm model,¹⁶ we investigated and compared the virulence of different, species-specific, bacterial biofilms by quantifying their effects on wound healing and the host inflammatory response. As a result, we have used our findings to highlight a previously underappreciated contributor to biofilm pathogenicity.

The current literature surrounding biofilm pathogenicity and virulence has focused on a variety of molecular pathways and bacterial species. In *S aureus*, many groups have focused on the accessory regulator protein *sarA* as a key mediator of biofilm formation. Beenken and colleagues³² demonstrated that mutation of *sarA* limited the development of *S aureus* biofilm in vitro, while the addition of a mutation in another accessory gene regulator, *agr*, did not incrementally effect the end phenotype. More recently, Weiss and associates³³ demonstrated that in a catheter-

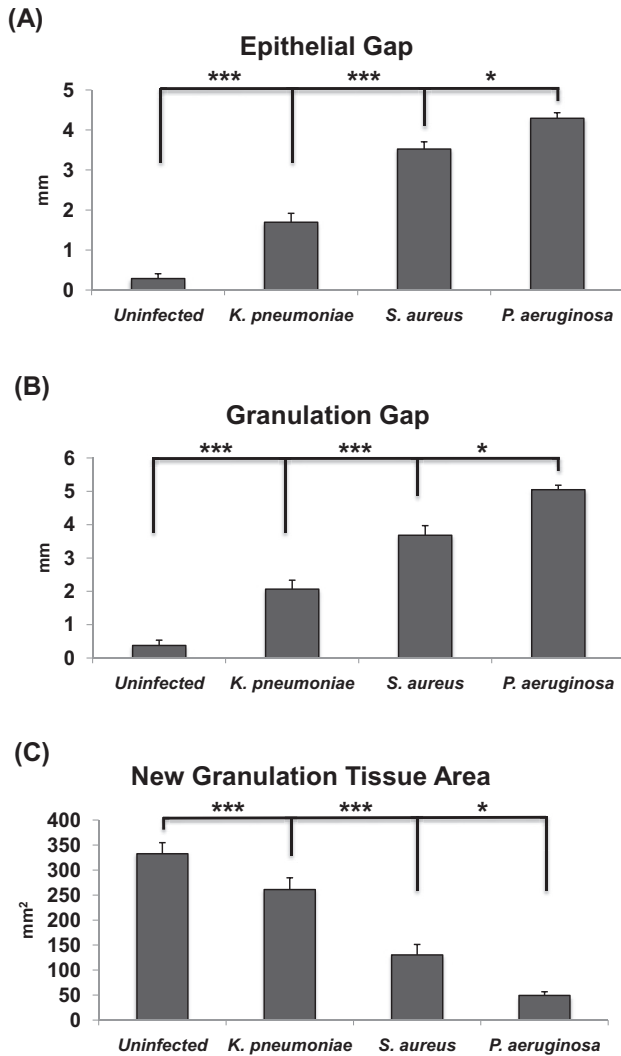


Figure 3. Comparison of quantitative histologic parameters between the 3 bacterial species studied. Measurements of (A) epithelial and (B) granulation gaps and (C) new tissue granulation area revealed that *P. aeruginosa* wounds had significantly impaired healing compared with uninfected controls (***) $p < 0.001$, *K. pneumoniae* (***) $p < 0.001$, and *S. aureus* (*) $p < 0.05$ across all measured histologic parameters (n = 16 to 20 wounds/species).

associated in vitro biofilm model, mutation of *sarA* resulted in an increased susceptibility of in vitro biofilm to antibiotics. Meanwhile, a number of groups have continued to demonstrate the importance of quorum-sensing to *P. aeruginosa* virulence,^{21,30,40} although work from Schaber and coworkers⁴¹ indicates that even quorum-sensing deficient *P. aeruginosa* are capable of forming in vivo biofilms in a thermally injured mouse model. Nevertheless, the virulence of different bacterial species has never been directly compared, making it difficult to extrapolate these findings to polybacterial settings. In addition, as previously mentioned, there re-

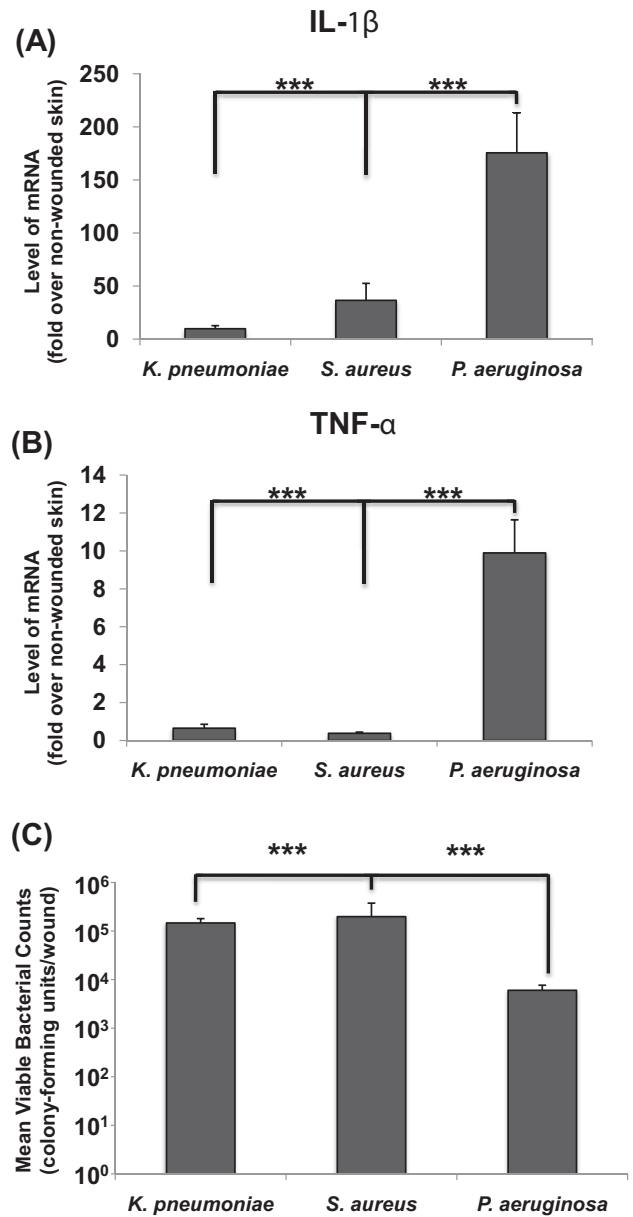


Figure 4. Comparison of inflammatory cytokine mRNA levels and viable bacterial counts in biofilm-infected wounds. *P. aeruginosa* wounds at postoperative day (POD) 6 demonstrated significantly higher levels of mRNA for inflammatory cytokines (A) interleukin (IL)-1 β and (B) tumor necrosis factor (TNF)- α as compared with *K. pneumoniae* and *S. aureus* wounds (***) $p < 0.001$; n = 8 to 10 wounds/species). (C) Bacterial counts were performed at POD 6 to ensure differences in inflammatory cytokine mRNA levels were not related to large differences in wound bacterial burden. *K. pneumoniae* and *S. aureus* biofilm-infected wounds revealed similar levels of bacterial counts. However, despite triggering a greater host inflammatory response, *P. aeruginosa* biofilm-infected wounds demonstrated significantly lower levels of viable bacteria relative to the other 2 species (***) $p < 0.001$; n = 8 to 10 wounds/group).

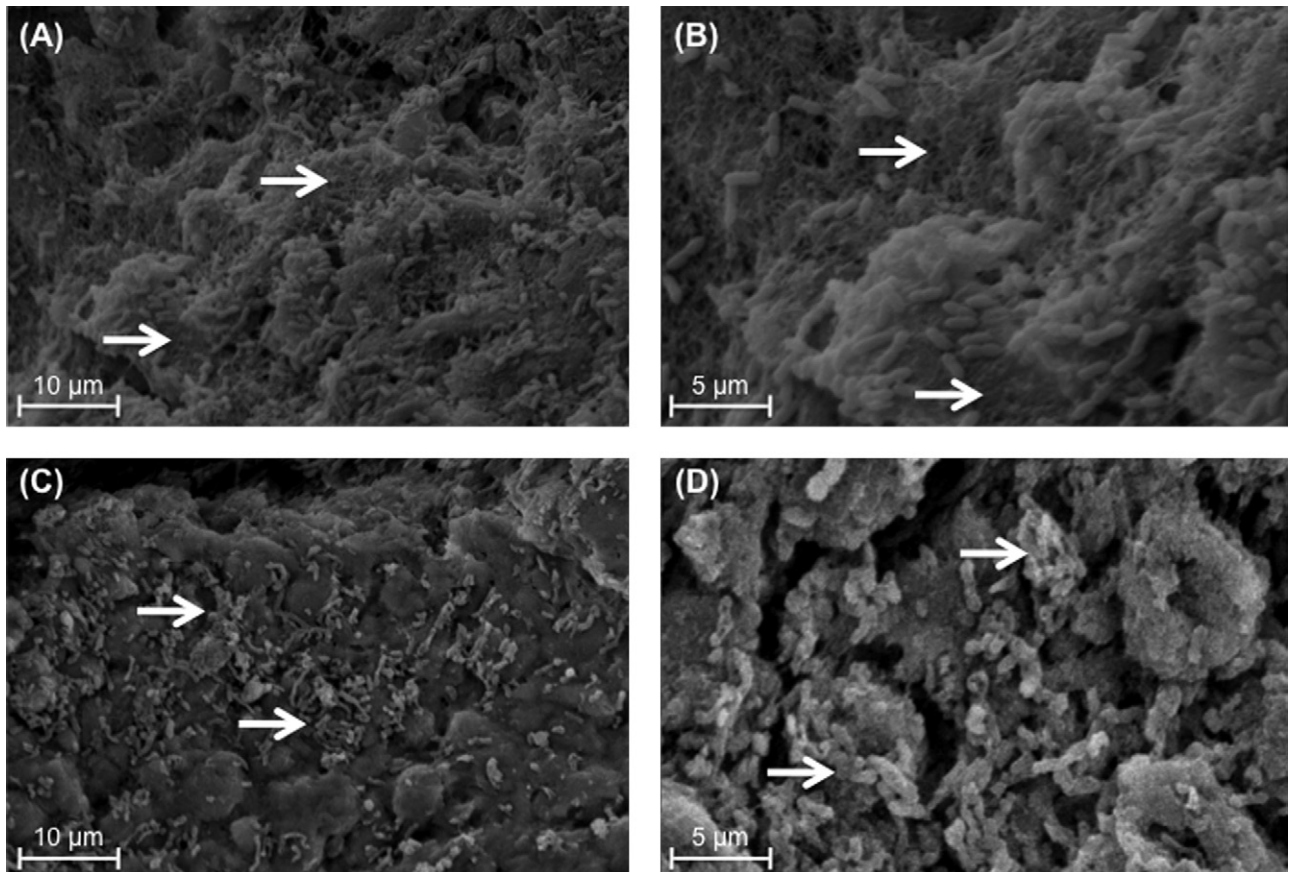


Figure 5. Scanning electron microscopy of *P aeruginosa* wild-type (PAO1) and mutant (*pelAps/BCD*) biofilm-infected wounds. Wild-type wounds (A and B) revealed large amounts of extracellular polymeric substance (EPS) matrix arranged in a lattice-like structure (arrows). In contrast, EPS-deficient mutant *pelAps/BCD* wounds (C and D) demonstrated minimal amounts of matrix between individual bacterial cells despite some evidence of clustering (arrows). The lack of EPS in *pelAps/BCD* wounds verified the phenotype that was expected morphologically.

mains little evidence to support the importance of the EPS to biofilm virulence. Early work by Deighton and colleagues²³ suggested that the extracellular “slime” of *S. epidermidis* biofilm-based catheter infections delayed the

clearance of *S. epidermidis* relative to biofilm-negative strains. In 2010, Borlee and associates⁴² reported on an adhesin molecule important to the structural integrity of *P aeruginosa* EPS, but did not extend these findings to its effect on

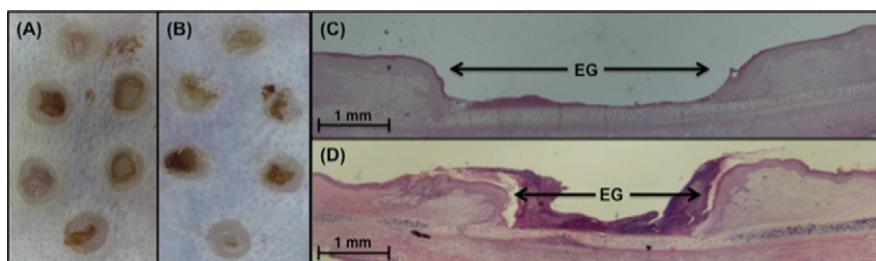


Figure 6. Gross appearance and histologic sections of (A and C) wild-type PAO1- and (B and D) mutant *pelAps/BCD*-infected wounds on postoperative (POD) 12 before harvest. (B) Wounds infected with *pelAps/BCD* appeared to have consistently smaller gaps in epithelial and granulation tissue compared with (A) PAO1, indicating a decreased ability to impair wound healing. Histologic sections stained with hematoxylin and eosin at POD 12 showed that (D) mutant *pelAps/BCD* wounds had improved healing compared with (C) PAO1 wounds, including a smaller epithelial gap, correlating with their gross appearance. (Magnification $\times 20$) EG, epithelial gap.

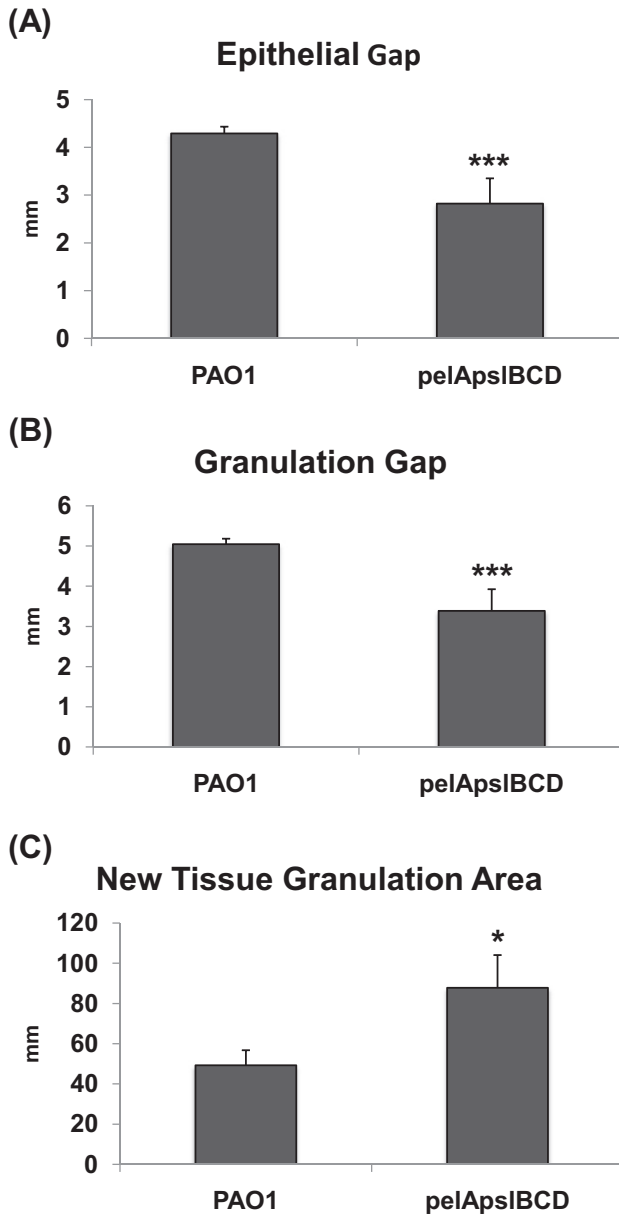


Figure 7. Comparison of quantitative histologic parameters between wild-type PAO1 and mutant *pelApsiBCD* wounds. Mutant *pelApsiBCD* biofilm-infected wounds had significantly smaller (A) epithelial and (B) granulation gaps (***) $p < 0.0001$) and larger amount of (C) new granulation tissue (* $p < 0.05$; $n = 16$ to 20 wounds/strain).

P aeruginosa virulence. Consequently, there remains limited evidence on the importance of the EPS to biofilm pathogenicity, particularly in vivo.

Through this study, we have demonstrated measurable differences in biofilm virulence between *K pneumoniae*, *S aureus*, and *P aeruginosa*. An analysis of their effects on wound healing inhibition and the host inflammatory response revealed that *P aeruginosa* biofilm was the most

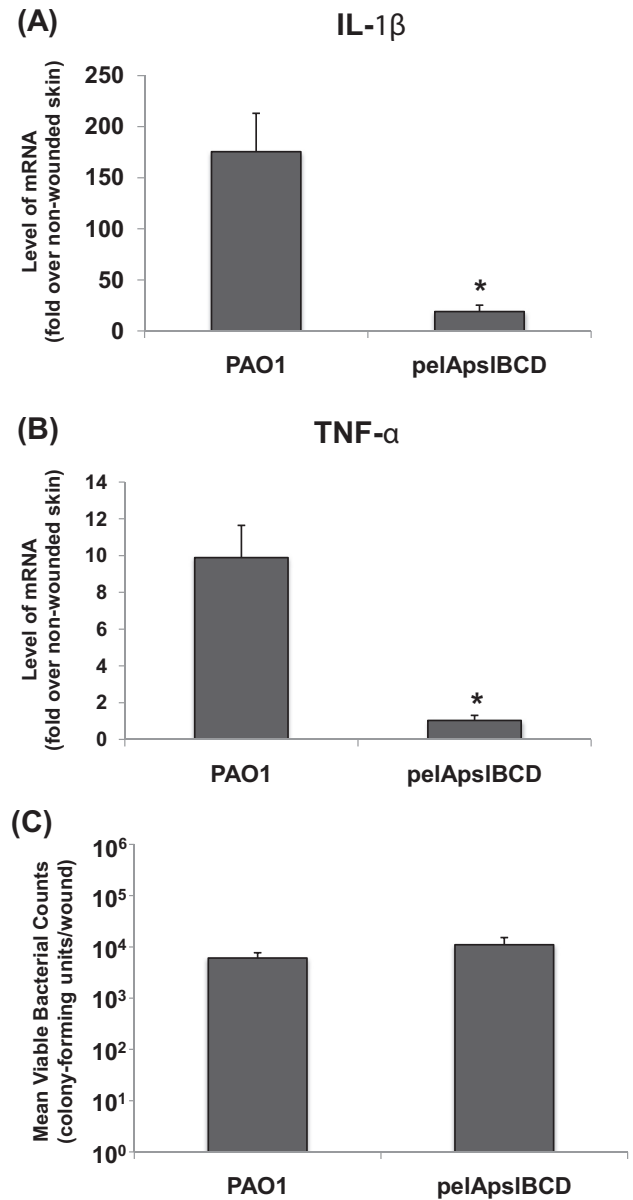


Figure 8. Comparison of inflammatory cytokine mRNA levels and viable bacterial counts between wild-type PAO1 and mutant *pelApsiBCD* wounds. On postoperative day (POD) 6, mutant *pelApsiBCD* wounds demonstrated significantly lower levels of mRNA for cytokines (A) interleukin (IL)-1 β and (B) tumor necrosis factor (TNF)- α in comparison with wild-type PAO1, indicating that the extracellular polymeric substance (EPS)-deficient mutant triggered a decreased host inflammatory response (* $p < 0.05$; $n = 8$ to 10 wounds/strain). Verifying that the differences in inflammatory response were not related to differences in bacterial burden, mutant *pelApsiBCD* wounds had similar levels of (C) viable bacteria in comparison with PAO1 wounds ($n = 8$ to 10 wounds/strain).

pathogenic species studied. In particular, *P aeruginosa* had the greatest effect on inflammatory cytokine expression despite the smallest number of viable bacteria. However,

visualization of biofilm morphology on SEM showed that *P aeruginosa* had the highest density of EPS among the 3 species, prompting additional investigation using an EPS-deficient *P aeruginosa* mutant. By observing a significant decrease in virulence from wild-type to mutant *P aeruginosa*, we concluded that the EPS is a critical factor in the heightened virulence of *P aeruginosa*.

Although several biofilm virulence factors have been identified for different bacterial species, no studies have performed a direct comparison of species-specific virulence using multiple endpoints. Through quantification of these differences, we have established a hierarchy of biofilm virulence among these common pathogens. These findings have multiple clinical implications for biofilm-infected chronic wounds. Previous work from our group has demonstrated that frequent, aggressive, and multimodal clinical wound care against *P aeruginosa* biofilm is necessary to obtain significant improvements in wound healing and bacterial viability.⁴³ However, wounds infected with a less virulent bacterial species, such as *K pneumoniae*, may not require the same level of treatment. Differentiating the severity of chronic wound infections based on the infecting bacteria's virulence can help with the development of appropriate treatment plans, while also allowing for prioritization of wound care resources. In addition, given that most chronic wounds are infected by multiple bacterial species,^{2,4,7,15} understanding the contribution of each bacterial species to the overall infection is important for developing effective therapeutics against a polybacterial biofilm. These differences in virulence may also have an impact on the dynamics of a polybacterial infection by influencing the interactions that occur between bacterial species.

It is particularly notable that *K pneumoniae* was found to have the least virulent wound biofilm among species studied, given its pathogenicity in other organ systems.⁴⁴ Although not a common chronic wound pathogen, relative to *S aureus* and *P aeruginosa*, multidrug resistant strains of *K pneumoniae* have been identified in the infected wounds of soldiers returning from war in Iraq.⁴⁵ Despite the tissue damage seen in these wounds, our results using one of these clinically isolated strains indicate that these strains may trigger only a modest amount of healing impairment when in a monospecies infection. Therefore, one can speculate that the detrimental effects of *K pneumoniae* wound biofilm may actually be potentiated in a polymicrobial environment, such as that within an infected war wound. However, additional work is needed to understand these dynamic differences in the pathogenicity of a single bacterial species.

The high level of virulence exhibited by *P aeruginosa* was investigated through the use of an EPS-deficient mutant

strain of *P aeruginosa*. Recent literature has focused on quorum-sensing between *P aeruginosa* cells as a critical virulence factor,^{2,21,29,30} with the goal of developing therapeutics aimed at disrupting these cell-to-cell signaling pathways. However, there is little evidence to date that *P aeruginosa* EPS may also be an important mediator of its biofilm pathogenicity. Qin and coworkers⁴⁶ used the same mutant, *pelApslBCD*, to demonstrate that extracellular products within the supernatant of *P aeruginosa* are capable of disrupting *S. epidermidis* biofilm formation in vitro. Meanwhile Koo and associates⁴⁷ suggest that in oral biofilms, the EPS of *S mutans* can contribute to the pathogenesis of dental caries. In similar fashion, our results indicate that *P aeruginosa* deficient in EPS triggers a milder inflammatory response and a decreased impairment in wound healing when compared with wild-type. As previously discussed, the EPS provides a number of protective advantages against host defense mechanisms,^{22,25-28} which may provide an explanation for our findings. However, EPS consists of a diverse group of polymers, including polysaccharides, proteins, and nucleic acids.⁴⁸ This complexity indicates that it may act as a platform for dynamic signaling pathways rather than being solely a physical barrier. Furthermore, the high density of EPS seen in *P aeruginosa* biofilms on SEM, as compared with *K pneumoniae* and *S aureus*, may further validate its contribution to the differences in virulence that we report. However, given that each species produces its own specific EPS using different substrates, it is difficult to validate this relationship without further molecular studies.

CONCLUSIONS

The potential importance of the EPS to biofilm virulence indicates a need for further investigation into therapeutics aimed at disrupting its dense structure. Traditional wound care methods, such as debridement and lavage, have been shown to disturb *P aeruginosa* biofilm structure in previous iterations of our model.⁴³ However, without an aggressive regimen of frequent multimodality treatments, the biofilm EPS appears to regain its structure, and therefore presumably some of its virulence as well. Others have demonstrated that topical formulations of specific D-amino acids are effective in both preventing biofilm growth and triggering disassembly of biofilm structure in both *S aureus* and *P aeruginosa*.^{48,49} Treatments such as these not only weaken the physical barrier that the EPS provides, but may also reduce the effectiveness of any innate virulence factors that it may have. Although biofilm research continues to focus on mechanisms of virulence such as quorum sensing, we believe our findings highlight the importance of a renewed interest in understanding, and targeting, the molecular pathways associated with biofilm EPS.

We acknowledge that despite our novel findings, our study is limited by a lack of understanding of species-specific biofilm virulence at a molecular level. Instead, we have performed work that has outlined the dynamics of different species' biofilms, while preliminarily implicating the EPS as a potential target warranting future investigation. However, we chose to not expand our initial investigation of EPS to *S aureus* and *K pneumoniae* given the ready availability of an EPS-deficient *P aeruginosa* mutant. Understanding the individual role of EPS in different species of bacteria will be crucial in implicating it as a therapeutic target. Furthermore, we did not perform additional experiments to compare the importance of EPS to other virulence factors, such as the well-known quorum-sensing pathways of *P aeruginosa*. However, with the power of this in vivo model, we have created a solid foundation for being able to compare different virulence factors whose end effects might otherwise be difficult to differentiate from one another. As our understanding of biofilm virulence continues to grow, our ability to counteract its destructive effects on chronic wounds will also improve. Future studies extending from this work will help further define the relationships and mechanisms introduced here, setting the stage for a new era of microbiologic therapeutics.

Author Contributions

Study conception and design: Seth, Geringer, Galiano, Leung, Mustoe, Hong

Acquisition of data: Seth, Geringer

Analysis and interpretation of data: Seth, Geringer, Galiano, Leung, Mustoe, Hong

Drafting of manuscript: Seth, Geringer

Critical revision: Seth, Geringer, Galiano, Leung, Mustoe, Hong

Acknowledgement: The authors would like to thank Anand N Gurjala for his contributions to the development of the model for this study.

REFERENCES

1. Fleck CA. Fighting infection in chronic wounds. *Adv Skin Wound Care* 2006;19:184–188.
2. Lindsay D, von Holy A. Bacterial biofilms within the clinical setting: what healthcare professionals should know. *J Hosp Infect* 2006;64:313–325.
3. Parsek MR, Singh PK. Bacterial biofilms: an emerging link to disease pathogenesis. *Annu Rev Microbiol* 2003;57:677–701.
4. Edwards R, Harding KG. Bacteria and wound healing. *Curr Opin Infect Dis* 2004;17:91–96.
5. James GA, Swogger E, Wolcott R, et al. Biofilms in chronic wounds. *Wound Repair Regen* 2008;16:37–44.
6. Dowd SE, Sun Y, Secor PR, et al. Survey of bacterial diversity in chronic wounds using pyrosequencing, DGGE, and full ribosome shotgun sequencing. *BMC Microbiol* 2008;6:43.
7. Gjodsbol K, Christensen JJ, Karlsmark T, et al. Multiple bacterial species reside in chronic wounds: a longitudinal study. *Int Wound J* 2006;3:225–231.
8. Gordo A, Scuffham P, Shearer A, et al. The healthcare costs of diabetic peripheral neuropathy in the US. *Diabetes Care* 2003;26:1790–1795.
9. Carter MJ, Warriner RA 3rd. Evidence-based medicine in wound care: time for a new paradigm. *Adv Skin Wound Care* 2009;22:12–16.
10. Krasner D. Painful venous ulcers: themes and stories about their impact on quality of life. *Ostomy Wound Management* 1998;44:38–49.
11. Beckrich K, Aronovitch SA. Hospital-acquired pressure ulcers: a comparison of costs in medical vs. surgical patients. *Nurs Econ* 1999;17:263–271.
12. Perencevich EN, Sands KE, Cosgrove SE, et al. Health and economic impact of surgical site infections diagnosed after hospital discharge. *Emerg Infect Dis* 2003;9:196–203.
13. Ramsey SD, Newton K, Blough D, et al. Patient-level estimates of the cost of complications in diabetes in a managed-care population. *Pharmacoeconomics* 1999;16:285–295.
14. Ramsey SD, Newton K, Blough D, et al. Incidence, outcomes, and cost of foot ulcers in patients with diabetes. *Diabetes Care* 1999;22:382–387.
15. Burmolle M, Thomsen TR, Fazli M, et al. Biofilms in chronic infections - a matter of opportunity - monospecies biofilms in multispecies infections. *FEMS Immunol Med Microbiol* 2010;59:324–336.
16. Gurjala AN, Geringer MR, Seth AK, et al. Development of a novel, highly quantitative in vivo model for the study of biofilm-impaired cutaneous wound healing. *Wound Repair Regen* 2011;19:400–410.
17. Davis SC, Ricotti C, Cazzaniga A, et al. Microscopic and physiologic evidence for biofilm-associated wound colonization in vivo. *Wound Repair Regen* 2008;16:23–29.
18. Schierle CF, De la Garza M, Mustoe TA, et al. Staphylococcal biofilms impair wound healing by delaying reepithelialization in a murine cutaneous wound model. *Wound Repair Regen* 2009;17:354–359.
19. Rashid MH, Rumbaugh K, Passador L, et al. Polyphosphate kinase is essential for biofilm development, quorum sensing, and virulence of *Pseudomonas aeruginosa*. *Proc Natl Acad Sci U S A* 2000;97:9636–9641.
20. Zhao G, Hochwalt PC, Usui ML, et al. Delayed wound healing in diabetic (db/db) mice with *Pseudomonas aeruginosa* biofilm challenge: a model for the study of chronic wounds. *Wound Repair Regen* 2010;18:467–477.
21. Nakagami G, Sanada H, Sugama J, et al. Detection of *Pseudomonas aeruginosa* quorum sensing signals in an infected ischemic wound: An experimental study in rats. *Wound Repair Regen* 2008;16:30–36.
22. Shiau AL, Wu CL. The inhibitory effect of *Staphylococcus epidermidis* slime on the phagocytosis of murine peritoneal macrophages is interferon independent. *Microbiol Immunol* 1998;42:33–40.
23. Deighton MA, Borland R, Capstick JA. Virulence of *Staphylococcus epidermidis* in a mouse model: significance of extracellular slime. *Epidemiol Infect* 1996;117:267–280.
24. Pihl M, Chavez de Paz LE, Schmidtchen A, et al. Effects of clinical isolates of *Pseudomonas aeruginosa* on *Staphylococcal*

- epidermidis biofilm formation. *FEMS Immunol Med Microbiol* 2010;59:504–512.
25. Percival SL, Bowler PG. Biofilms and their potential role in wound healing. *Wounds* 2004;16:234–240.
 26. Johnson GM, Lee DA, Regelman WE, et al. Interference with granulocyte function by *Staphylococcus epidermidis* slime. *Infect Immun* 1986;54:13–20.
 27. Lewis K. Riddle of biofilm resistance. *Antimicrob Agents Chemother* 2001;45:999–1007.
 28. Shigeta M, Tanaka G, Komatsuzawa H, et al. Permeation of antimicrobial agents through *Pseudomonas aeruginosa* biofilms: A simple method. *Chemotherapy* 1997;43:340–345.
 29. Davies DG, Parsek MR, Pearson JP, et al. The involvement of cell-to-cell signals in the development of a bacterial biofilm. *Science* 1998;280:295–298.
 30. Nakagami G, Morohoshi T, Ikeda T, et al. Contribution of quorum sensing to the virulence of *Pseudomonas aeruginosa* in pressure ulcer infection in rats. *Wound Repair Regen* 2011;19:214–222.
 31. Kong K, Vuong C, Otto M. *Staphylococcus* quorum sensing in biofilm formation and infection. *Int J Med Microbiol* 2006;296:133–139.
 32. Beenken KE, Blevins JS, Smeltzer MS. Mutation of *sarA* in *Staphylococcus aureus* limits biofilm formation. *Infect Immun* 2003;71:4206–4211.
 33. Weiss EC, Spencer HJ, Daily SJ, et al. Impact of *sarA* on antibiotic susceptibility of *Staphylococcus aureus* in a catheter-associated in vitro model of biofilm formation. *Antimicrob Agents Chemother* 2009;53:2475–2482.
 34. Yarwood JM, Bartels DJ, Volper EM, Greenberg EP. Quorum sensing in *Staphylococcus aureus* biofilms. *J Bacteriol* 2004;186:1838–1850.
 35. Rice KC, Mann EE, Endres JL, et al. The *cidA* murein hydrolase regulator contributes to DNA release and biofilm development in *Staphylococcus aureus*. *Proc Natl Acad Sci U S A* 2007;104:8113–8118.
 36. Vuong C, Voyich JM, Fischer ER, et al. Polysaccharide intercellular adhesin (PIA) protects *Staphylococcus epidermidis* against major components of the human innate immune system. *Cell Microbiol* 2004;6:269–275.
 37. Jesaitis AJ, Franklin MJ, Berglund D, et al. Compromised host defense on *Pseudomonas aeruginosa* biofilms: characterization of neutrophil and biofilm interactions. *J Immunol* 2003;171:4329–4339.
 38. Jensen PO, Bjarnsholt T, Phipps R, et al. Rapid necrotic killing of polymorphonuclear leukocytes is caused by quorum-sensing-controlled production of rhamnolipid by *Pseudomonas aeruginosa*. *Microbiology* 2007;153:1329–1338.
 39. Zhao LL, Davidson JD, Wee SC, et al. Effect of hyperbaric oxygen and growth factors on rabbit ear ischemic ulcers. *Arch Surg* 1994;129:1043–1049.
 40. Rumbaugh KP, Diggle SP, Watters CM, et al. Quorum sensing and the social evolution of bacterial virulence. *Curr Biol* 2009;19:341–345.
 41. Schaber JA, Triffo WJ, Suh SJ, et al. *Pseudomonas aeruginosa* forms biofilms in acute infection independent of cell-to-cell signaling. *Infect Immun* 2007;75:3715–3721.
 42. Borlee BR, Goldman AD, Murakami K, et al. *Pseudomonas aeruginosa* uses a cyclic-di-GMP-regulated adhesin to reinforce the biofilm extracellular matrix. *Mol Microbiol* 2010;75:827–842.
 43. Seth AK, Geringer MR, Gurjala AN, et al. Treatment of *Pseudomonas aeruginosa* biofilm-infected wounds with clinical wound care strategies: A quantitative study using an in vivo rabbit ear model. *Plast Reconstr Surg* 2012;129:262e–274e.
 44. Podschun R, Ullmann U. *Klebsiella* spp. as nosocomial pathogens: epidemiology, taxonomy, typing methods, and pathogenicity factors. *Clin Microbiol Rev* 1998;11:589–603.
 45. Calhoun JH, Murray CK, Manring MM. Multidrug-resistant organisms in military wounds from Iraq and Afghanistan. *Clin Orthop Relat Res* 2008;466:1356–1362.
 46. Qin Z, Yang L, Qu D, et al. *Pseudomonas aeruginosa* extracellular products inhibit staphylococcal growth, and disrupt established biofilms produced by *Staphylococcus epidermidis*. *Microbiology* 2009;155:2148–2156.
 47. Koo H, Xiao J, Klein MI. Extracellular polysaccharides matrix – An often forgotten virulence factor in oral biofilm research. *Int J Oral Sci* 2009;1:229–234.
 48. Hochbaum AI, Kolodkin-Gal I, Foulston L, et al. Inhibitory effects of D-amino acids on *Staphylococcus aureus* biofilm development. *J Bacteriol* 2011;193:5616–5622.
 49. Kolodkin-Gal I, Romero D, Cao S, et al. D-amino acids trigger biofilm disassembly. *Science* 2010;328:627–629.